ACS OMEGA

Article

Cite This: ACS Omega 2018, 3, 15464−15470

http://pubs.acs.org/journal/acsodf

Reduced Graphene Oxide-Oligonucleotide Interfaces: Understanding Based on Electrochemical Oxidation of Guanines

Anjong Florence Tikum, Jeong Won Ko, Soojin Kim, and Jinheung Kim*

Department of Chemistry and Nano Science, Ewha Womans University, Seoul 120-750, Korea

Supporting Information

ABSTRACT: Investigation into the interactions between biomolecules DNA/RNA and carbon nanomaterials is very important for applications in bioassays and bioanalysis. Graphene and graphene oxide (GO) have been successfully adopted by exploiting the binding affinity difference between single-stranded oligonucleotides (ssDNA) and double-stranded oligonucleotides (dsDNA) to graphene sheets. In this work, we describe the electrochemical DNA oxidation with $[Ru(bpy)_3]^{2+}$ to understand the interaction between dsDNA (and corresponding ssDNA) and reduced graphene oxide (rGO). The electrochemical oxidation rate of guanine bases of ssDNA bound to rGO by electrochemically generated $[Ru(bpy)_3]^{3+}$ was much slower than those unbound to rGO. Our study revealed that ssDNA constrained on rGO was significantly protected from the electron transfer to $[Ru(bpy)_3]^{3+}$ because of π,π-stacking interaction between nucleobases and rGO. On the other hand, the oxidation rates of 11-, 20-, and 27-mer dsDNA bound to rGO increased relative to those of dsDNA alone, demonstrating that the guanine bases of dsDNA on the interaction with rGO became more accessible to $[Ru(bpy)_3]^{3+}$. Our electrochemical data illustrated that dsDNA could be totally or partially dehybridized and bind to rGO to form ssDNA/rGO. Furthermore, absorption, circular dichroism spectra, and fluorescence measurements of ethidium bromide using ssDNA and dsDNA with rGO supported the dehybridization of dsDNA in the presence of rGO.

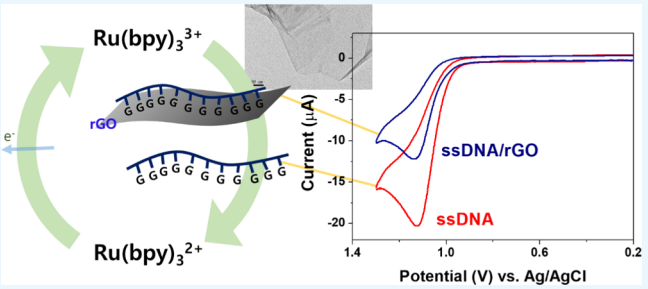

1. INTRODUCTION

The nanobio interfaces between nanomaterials and oligonucleotides have been fabricated and studied for fundamental significance and practical importance in materials science, biosensing, and biomedicine.[1−3] Recently, the integration of single-stranded and duplex DNA with nanomaterials, such as carbon nanotubes (CNT), graphene, graphene oxides (GO), and metal nanoparticles, has been substantially advanced.[1,2] For example, single-stranded DNA (ssDNA) was shown to adsorb on CNT, thereby enhancing the water solubility of CNTs.[4,5] DNA-/CNT-based devices were developed for biosensing and biomedical applications.[5,6] In addition, ssDNA was used to wrap on CNTs and then separate metallic CNT.[7]

Luminescence and electrochemical methods have been often used to study the interaction of DNA with carbon nanomaterials such as CNT, graphene, and GO. Among these studies, the interaction of DNA with GO was investigated with great interest. In recent works, ssDNA interacted strongly with graphene or GO, while double-stranded DNA (dsDNA) and folded ssDNA (such as G-quadruplex and hairpin structures) showed much lower affinity.[8−11] Overall, ssDNA readily adsorbed onto graphene by π,π-stacking interactions between graphene and nucleobases, which were supported by molecular simulations about the fundamental interactions between graphene materials and ssDNA.[12] However, the interactions between dsDNA and carbon nanomaterials need to be studied more, even though dsDNA interacts weakly with graphene and GO. Because of these unique interaction properties of ssDNA and dsDNA with graphene complexes, the application of graphene materials in biosensing and other bioengineering has recently attracted significant attention. For examples, complexes of ssDNA and GO were studied for new biomedical and bioassay platforms. DNA aptamers were well protected by GO from enzymatic cleavage during cellular transport.[9,13] Such different properties of ssDNA and dsDNA on the interaction with GO will be utilized more in DNA and protein analysis, gene and drug delivery, etc.

In the fluorescence studies, the most common strategy is to utilize fluorescence quenching of fluorophores covalently attached to a probe DNA on GO.[14,15] Then, the fluorescence of the probe is recovered after the formation of dsDNA with a target strand, which is detached from GO by hybridization. As reported elsewhere, the binding energy by base pairs in dsDNA was greater than the π,π-stacking interaction energy of a single-stranded oligonucleotide with GO. Therefore, their data were interpreted that the probe DNA strands on GO were desorbed to make double strands upon treatment with a target strand.

Received: August 16, 2018
Accepted: October 23, 2018
Published: November 14, 2018

DOI: 10.1021/acsomega.8b02063
ACS Omega 2018, 3, 15464−15470

However, GO was also reported to protect dsDNA from enzymatic digestion by forming dsDNA−GO complexes or a partial deformation of the double helix.[10−16] Therefore, further study is required to clarify the interactions of dsDNA with graphene and related nanomaterials.

Electrochemical studies of DNA nanomaterials have been reported to understand the interaction between DNA and nanomaterials and develop biosensors.[4,17,18] Many kinds of nanoparticles, such as metals, metal oxides, and semiconductor nanoparticles, have been used for constructing electrochemical sensors and biosensors. These nanoparticles play different roles in different sensing systems, such as the immobilization of biomolecules, the catalysis of electrochemical reactions, the enhancement of electron transfer between electrodes and biomolecules, the labeling of biomolecules, and even acting as a reactant.[19,20] Recently, we reported the direct electrochemical oxidation of oligonucleotides attached to Au nanoparticles (AuNPs) using a tris(2,2′-bipyridyl)ruthenium(II) complex, $Ru(bpy)_3^{2+}$ (bpy = 2,2′-bipyridine).[18] Depending on the size of AuNPs, the oxidation rates of the oligonucleotides varied because of different curvatures of ssDNA at the AuNP−water interfaces. In terms of carbon nanomaterials, carbon nanotubes having poor solubility in both aqueous and nonaqueous solvents were wrapped with 50-mer thymine bases to make carbon nanotubes (CNT) soluble in buffer solution, and the electrochemical oxidation of CNT was studied by a molecular Ru mediator. However, to the best of our knowledge, the oligonucleotide-mediated assembly of rGO, interactions of rGO especially with dsDNA, and electrochemical studies have not been reported up to now.

$Ru(bpy)_3^{2+}$ has been used in electrochemical studies to detect oligonucleotides.[18,21−23] As $Ru(bpy)_3^{2+}$ has the high oxidation potential at 1.1 V (vs Ag/AgCl), the electrochemically generated $Ru(bpy)_3^{3+}$ can oxidize guanine bases in DNA (shown in equations below). The oxidative scan of $Ru(bpy)_3^{2+}$ in the presence of DNA containing guanines affords big catalytic currents because of the oxidation of guanines to regenerate $Ru(bpy)_3^{2+}$ from $Ru(bpy)_3^{3+}$ during the scanning time. On the basis of this concept, detection of target DNA strands and adenosine using a specific DNA probe was reported in buffer solutions.[21−23] However, the electrochemical oxidation of ssDNA and dsDNA in the presence of graphene nanomaterials has not been reported up to now to understand their interaction properties.

$$Ru(bpy)_3^{2+} \rightarrow Ru(bpy)_3^{3+} + e^-$$

$$Ru(bpy)_3^{3+} + DNA \rightarrow Ru(bpy)_3^{2+} + DNA_{oxidized}$$

Herein, we first report the electrochemical study to understand the interaction of single- and double-stranded oligonucleotides with rGO and behavior of oligonucleotides at the rGO−water interface. The oxidation rate of guanine bases in DNA by $[Ru(bpy)_3]^{3+}$ slowed down as ssDNA was adsorbed on rGO. On the basis of our electrochemical and spectroscopic studies, we found that dsDNA was significantly dehybridized on the interaction with rGO. We believe that this work could help to understand the properties of such DNA−rGO hybrid materials and thus will advance the research of DNA−graphene materials for applications in biosensors and bionanotechnology.

2. RESULTS AND DISCUSSION

Three different DNA sequences containing guanine bases were used to prepare DNA−rGO hybrid materials and study their interaction and electrochemical properties (Table 1). The

Table 1. DNA Sequences and Abbreviations Used in This Study

abbreviation	oligonucleotide sequences
G11	5′-GGG GGG GGG GG
C11	5′-CCC CCC CCC CC
G20	5′-GGG GGG GGG GGG GGG GGG GG
C20	5′-CCC CCC CCC CCC CCC CCC CC
B24G3	5′-AAA TAT ATA TAT GGG ATA TAT ATA AAA
B24C3	5′-TTT TAT ATA TAT CCC ATA TAT ATA TTT

electrochemical oxidation of single-stranded G11 was first studied with $Ru(bpy)_3^{2+}$ (bpy = 2,2′-bipyridine) in the absence of reduced graphene oxide (rGO) in a phosphate buffer at room temperature. G11 alone afforded a big oxidative current enhancement at 1.1 V at a scan rate of 25 mV/s, as reported with other oligonucleotides containing guanine (Figures 1a and S1). The current enhancement in the presence of G11 is due to the catalytic oxidation of guanine bases by $Ru(bpy)_3^{3+}$ electrogenerated in the process of oxidative scan. However, the catalytic current with dsDNA G11//C11 alone was lower than that with G11 because the accessibility of the Ru mediator to the guanines of the double-stranded DNA became lower in solution, as reported elsewhere (Figures 1b and S1).[21−23] The other strands, G20 and B24G3, also showed similar trends (Figure S1). As reported earlier, the number of guanines in oligonucleotides affected the catalytic current. The oxidative current with G20 turned out the biggest, followed by G11 and B24G3 (Figures S1 and S2).

Then, when G11 was incubated with rGO, it could interact with rGO by the π,π-stacking interaction and then the hybrid material G11/rGO was formed (Figure 2). Under the conditions in Figure 1, the amount of rGO was for a compete adsorption of DNA based on the electrochemical and emission measurements. We tried to observe a difference in the guanine oxidation current by $Ru(bpy)_3^{3+}$ between G11 and G11/rGO. The oxidation current of G11/rGO significantly decreased (Figure 1a). The current decreased progressively with increasing rGO (Figure S3). Because rGO was not oxidized by $Ru(bpy)_3^{3+}$ under the conditions (Figure S4), the reduction of the catalytic current derived from a relatively slow electron transfer from the guanine bases of G11/rGO to $Ru(bpy)_3^{3+}$. The phosphate backbone of G11 in G11/rGO is directed to the aqueous solution, and the guanine bases are toward rGO for stacking interaction. Then, the electron transfer from the guanines of G11 to $Ru(bpy)_3^{3+}$ was slowed down because of the slow electron transfer rate due to the low accessibility to guanines. In a control experiment, C11/rGO prepared with C11 and rGO afforded no significant current increase. The catalytic current with G11/rGO was confirmed to derive from the oxidation of guanines, not rGO. However, it was reported that CNT wrapped with T50 was oxidized by electrochemically generated Ru(III) species having a lower redox potential than $Ru(bpy)_3^{2+}$, indicating the oxidation of CNT.[4] Therefore, our data demonstrate that rGO should be less easily oxidized than CNT because rGO was not oxidized by $Ru(bpy)_3^{3+}$.

Then, G11//C11 was used to observe changes in current when interacted with rGO. It was reported that ssDNA was

DOI: 10.1021/acsomega.8b02063
ACS Omega 2018, 3, 15464−15470

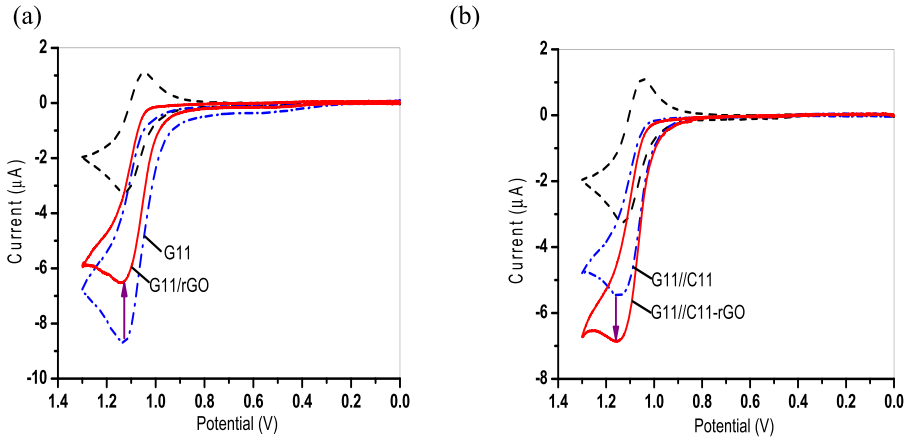

Figure 1. Electrochemical responses for (a) G11 (blue dash-dotted line) and G11/rGO (red solid line), and (b) G11//C11 (blue dash-dotted line) and G11//C11−rGO (red solid line) in phosphate buffer solution with 50 μM $Ru(bpy)_3^{2+}$. The cyclic voltammogram of 50 μM $Ru(bpy)_3^{2+}$ alone was plotted as a black dashed line. The stock solution of rGO was 0.6 mg/mL, and the scan rate was 25 mV/s. No current enhancement was observed for rGO alone when $Ru(bpy)_3^{2+}$ was used.

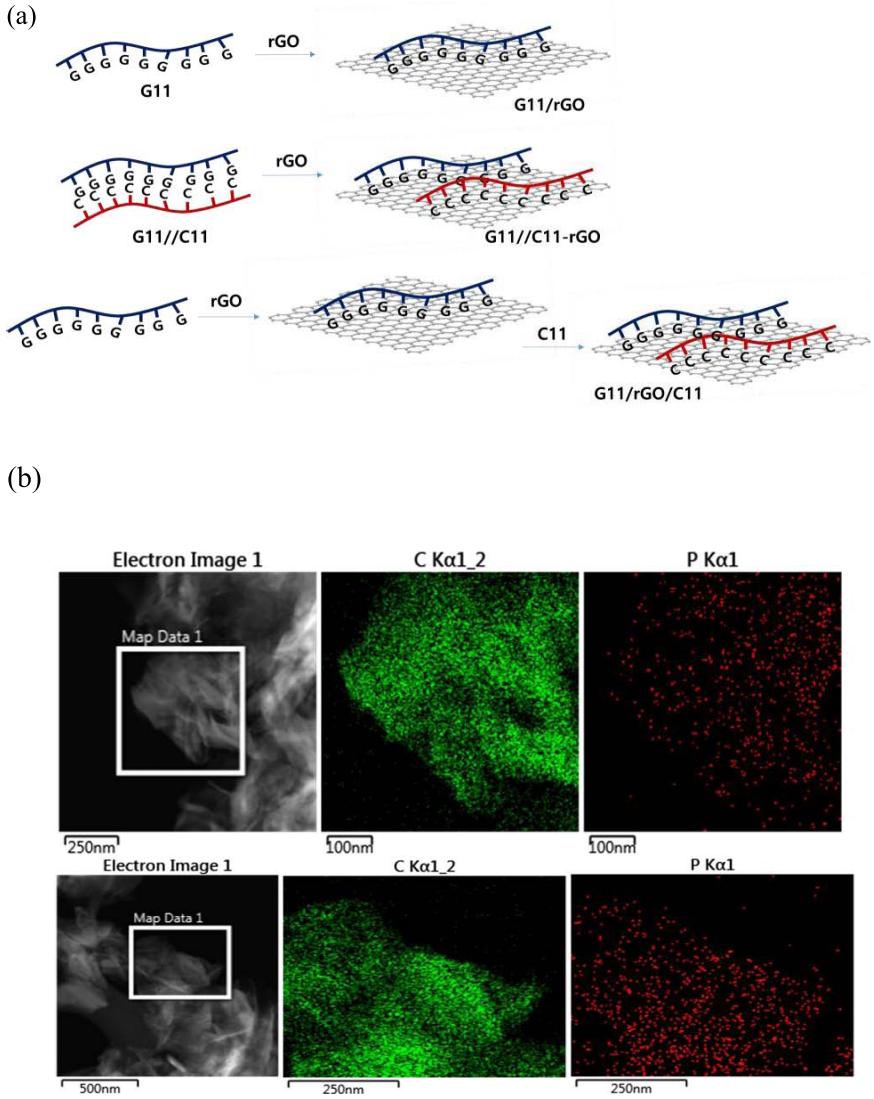

Figure 2. (a) Schematic illustration of the interactions between DNA and reduced graphene oxide, showing the formation of G11/rGO, G11/C11−rGO, and G11/rGO/C11. (b) Transmission electron microscopy (TEM) images of G11/rGO (top) and G11/C11−rGO (bottom), and the corresponding energy dispersive X-ray spectrometry (EDS) mapping images of C and P.

DOI: 10.1021/acsomega.8b02063
ACS Omega 2018, 3, 15464−15470

bound to GO with a high affinity, while dsDNA or well-folded ssDNA (such as G-quadruplex, etc.) exhibited much lower affinity. According to these observations, the current with G11//C11 would be expected to be almost the same as that with a mixture of G11//C11 and rGO because G11//C11 would remain the same even in the presence of rGO. In practice, when G11//C11 was treated with rGO, the current interestingly increased (Figure 1b). The current obtained with G11//C11−rGO was almost the same as that with G11/rGO. The current enhancement meant that G11//C11 was completely dehybridized and the dehybridized C11 and G11 were attached to rGO (Figure 2a). The TEM images of G11/rGO and G11/C11−rGO were obtained, and the corresponding EDS mapping images indicated the presence of DNA (Figure 2b). In a control experiment with a G11/rGO/C11 sample in which G11 was incubated first with rGO and then with C11, a similar current was obtained as that with G11//C11−rGO (Figure S5). These observations implied that the solvent accessibility of G11//C11 should be lower than that of G11//C11−rGO. It seems that the binding energy between G11 and C11 formed by hydrogen bonding would be lower than the π,π-stacking interaction energy between rGO and the single strands of G11 and C11. These results were somewhat different from those observed in other studies using fluorescence measurements, showing that dsDNA interacted more weakly with graphene and stayed without a change. Recently, the partial deformation of 21-mer dsDNA was also reported on the interaction with GO, on the basis of enzymatic activity studies of dsDNA.[16] The reasons for the different observations in the interactions of ssDNA and dsDNA with carbon nanomaterials might derive from the use of different graphene materials, such as graphene and GO in their studies, instead of rGO. Further detailed studies using carbon nanomaterials are needed to make two different observations clear.

Because the binding energy between two single strands of a dsDNA depends on the number of bases, 20- and 27-mer dsDNA, such as G20//C20 and B24G3//B24C3, were used in the presence of rGO for the electrochemical study. For both dsDNA, similar results were obtained in that the oxidative current with dsDNA increased on the interaction with rGO (Figures S6 and S7). These results demonstrate that the 20- and 27-mer dsDNA were also dehybridized on the interaction with rGO to afford the higher solvent accessibility to the Ru mediator. Especially, B24G3//B24C3 containing GGG in the middle of the sequence was also deformed with rGO and the GGG part of B24G3/rGO became more readily exposed to the solvent relative to those in dsDNA. These results indicated that the double-stranded DNA of 27-mer was also significantly dehybridized because of the π,π-stacking interaction with rGO.

Then, absorption spectra of G20, G20//C20, G20/rGO, and G20//C20−rGO were recorded to understand the interaction of DNA with rGO further and check the deformation of G20//C20 by rGO. When G20 was adsorbed on rGO, the absorbance of G20/rGO decreased at 260 nm relative to G20 alone, as reported in other studies with CNT and AuNPs (Figure 3a).[18,24] Absorption spectra of G20//C20 and G20//C20−rGO were also recorded to check the extent of dehybridization of G20//C20 in the presence of rGO (Figure 3b). The absorbance of G20//C20−rGO also decreased at 260 nm. However, the absorption spectrum of G20//C20−rGO was very similar to that observed with G11/rGO but exhibited a little higher absorbance at 260 nm. These

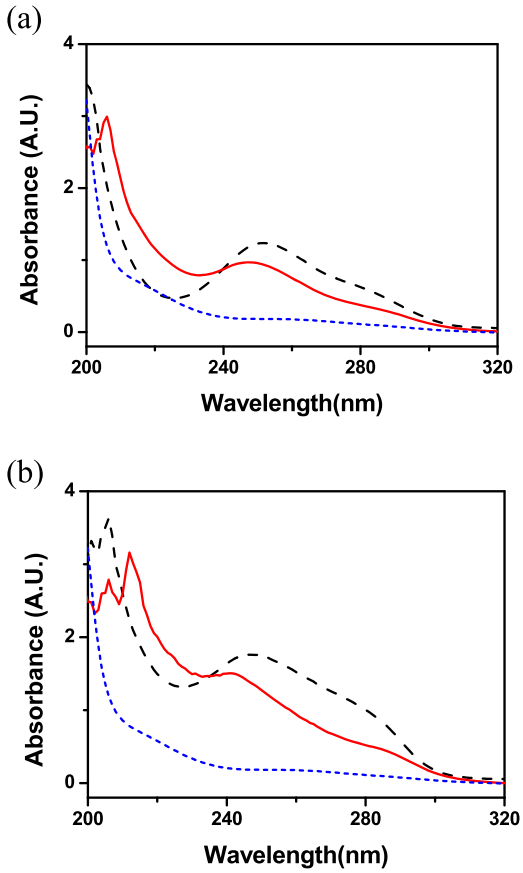

Figure 3. Absorption spectra of (a) 5 μM G20 (black dashed line), G20/rGO (red solid line), and rGO (blue dotted line), and (b) 5 μM G20//C20 (black dashed line), G20//C20−rGO (red solid line), and rGO (blue dotted line) in 0.1 M Na-phosphate buffer (pH 7.4).

results also supported that G20//C20 was deformed on the interaction with rGO and then two single strands would bind to rGO.

To study the interaction of duplex DNA with rGO further, circular dichroism (CD) spectra were investigated for B24G3//B24C3 and rGO. Duplex DNA had two peaks on the CD spectrum, a positive peak at about 275 nm and a negative peak at about 246 nm (Figure 4). Upon the addition

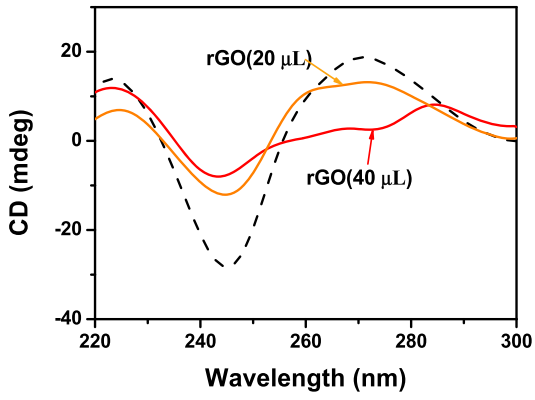

Figure 4. Circular dichroism (CD) spectra of B24G3//B24C3 (black dashed line) and B24G3//B24C3−rGO (20 μL rGO, orange solid line; 40 μL rGO, red solid line) in 0.1 M Na-phosphate buffer (pH 7.4).

DOI: 10.1021/acsomega.8b02063
ACS Omega 2018, 3, 15464−15470

of increasing amount of rGO (20 and 40 μL of a stock solution), a consistent decrease was seen both for the negative and the positive peak, indicating that the duplex DNA was dissociated. The CD spectrum of B24G3//B24C3−rGO sample was similar to that of B24G3/rGO, implying that dsDNA was dehybridized on the interaction with rGO. CD experiments with G20//C20 and rGO also afforded similar results (Figure S8). Such CD spectral changes were also observed with other dsDNA sequences with GO, which were interpreted as a partial deformation of dsDNA.[25,26]

In addition, photoluminescence (PL) study was carried out to understand further the interaction between dsDNA and rGO using the strong intercalating property of ethidium bromide (EtBr) into dsDNA. EtBr intercalated into dsDNA exhibits strong characteristic fluorescence. The PL spectra are recorded for EtBr alone, and EtBr with rGO, G20, G20//C20, and G20//C20−rGO (Figure 5). G20//C20 treated with EtBr

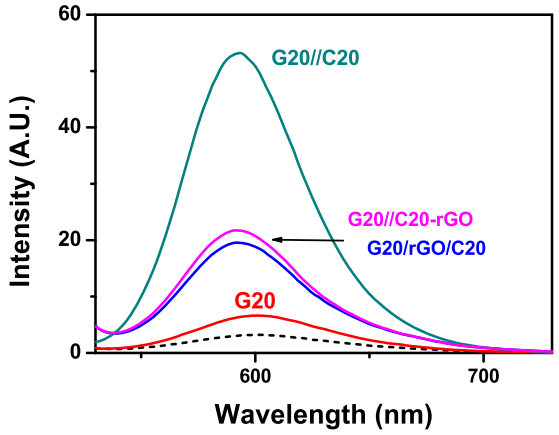

Figure 5. Photoluminescence spectra of ethidium bromide (EtBr) alone (black dotted line), G20 (red), G20//C20 (green), G20//C20−rGO (purple), and G20/rGO/C20 (blue) in 0.1 M Na-phosphate buffer (pH 7.4).

showed a strong emission at 590 nm on excitation at 480 nm, as expected from a well-established intercalation property of EtBr into dsDNA. EtBr alone had no significant emission in buffer solution, and G20 with EtBr afforded much smaller intensity than that of G20//C20. G20//C20−rGO also afforded a much lower emission, relative to that with G20//C20. The lower intensity with dsDNA in the presence of rGO could be interpreted as the conformational change of dsDNA on the interaction with rGO, which leads to the deformation of the duplex DNA. In a control experiment, the emission spectrum of G20−rGO−C20 was almost the same as that obtained with G20//C20−rGO. These data demonstrated that G20//C20 was dehybridized and the single-stranded G20 and C20 were adsorbed on rGO by π,π-interaction.

3. CONCLUSIONS

On the basis of this study, we found that single-stranded DNA interacted strongly with rGO to form stable ssDNA/rGO hybrid materials in aqueous solution and ssDNA bound to rGO was effectively protected from guanine oxidation by electrochemically generated $[Ru(bpy)_3]^{3+}$. Such strong interaction of ssDNA with rGO also derived from π,π-stacking interaction well reported in other studies with graphene and GO.[11,12] The current enhancement of dsDNA−rGO solution relative to dsDNA alone implied that dsDNA was deformed and would bind to rGO as single strands. In studies reporting no significant interaction of dsDNA with graphene-based materials, and desorption of ssDNA from graphene materials by a complementary strand, various lengths of DNA were used, from 12-mer to 50-mer oligonucleotides.[9,11,12,16,27] Consequently, it seems not just a matter of DNA length. Several factors, such as DNA sequence, length, hybridization, heterogeneous structure of graphene materials, etc., should be considered for complete understanding of such interesting and complex biointerfacial systems. Further studies are necessary to understand interaction properties between DNA and graphene-based materials in aqueous solution.

In addition, absorption, CD, and fluorescence studies suggested that ssDNA and dsDNA of 11-, 20-, and 27-mer oligonucleotides would be promptly bound to rGO forming strong noncovalent interactions and a significant dehybridization of dsDNA occurs in the presence of rGO. Under the similar conditions in aqueous solutions, we observed that the oxidation potential of rGO was much higher than that of CNT.[4] As shown in our findings, conformational changes of DNA on the interaction with nanomaterials can afford different electrochemical signals to have potential for biomolecular recognition and sensing because graphene-based materials have been utilized in various electrochemical sensors. This study connects the biomolecule, DNA, with a two-dimensional carbon nanomaterial, reduced graphene oxide, demonstrating that the unique electrochemical properties of the DNA/rGO platform may inspire applications in biotechnology, biosensors, and biomedical research works.

4. EXPERIMENTAL SECTION

4.1. Materials and Instrumentation. Water was purified with a Milli-Q purification system. Oligonucleotides were purchased from GenoTec Inc. (Deajon, Korea) and purified by high performance liquid chromatography (Youngin Instrument, Korea, Acme 9000) using a Thermo Hypersyl Gold Column (0.46 × 25 cm^2). The oligonucleotide concentrations were measured on a BioSpec-nano spectrophotometer (220 V, 40VA Shimadzu, Japan). The working electrode was tin-doped indium oxide (ITO) obtained from Delta Technology, Inc. The ITO electrodes were cleaned by sequential 10 min sonications in Alkonox, 95% ethanol, and water twice, and finally the desired buffer. $[Ru(bpy)_3]Cl_2$ was purchased from Sigma-Aldrich. Reduced graphene oxide (rGO) was prepared using graphene oxide (GO) obtained from a graphite powder using a modified Hummers method.[28−30]

Voltammetry was carried out using a CH instrument galvanostat/potentiostat (CHI630C) with a single-compartment voltammetric cell equipped with the ITO working electrode (area = 0.32 cm^2), a Pt wire counter electrode, and an Ag/AgCl reference electrode. Circular dichroism (CD) measurements were performed with a JASCO J-810 spectrometer with temperature control at room temperature, unless otherwise specified. Samples were freshly prepared using 0.1 M sodium phosphate buffer (SPB, pH 7.4). UV−vis measurements were recorded on a Hewlett-Packard 8453 spectrophotometer.

4.2. Preparation of DNA−rGO. To prepare DNA−rGO materials, the solutions of oligonucleotides and rGO of appropriate concentrations were incubated for 15−30 min at room temperature in 0.1 M SPB (pH 7.4) with 50 mM NaCl right before each experiment.

DOI: 10.1021/acsomega.8b02063
ACS Omega 2018, 3, 15464−15470

4.3. Electrochemical Oxidation of DNA and DNA–rGO. A buffer solution containing 50 μM $Ru(bpy)_3^{2+}$ and oligonucleotides was scanned at 25 mV/s from 0.0 to 1.3 V (vs Ag/AgCl). A freshly cleaned ITO electrode was used for each experiment. Before each experiment with rGO, the DNA was mixed with different amounts of rGO and incubated for 15–30 min. Then, $Ru(bpy)_3^{2+}$ (50 μM) was added right before each measurement.

4.4. UV–Vis Measurements. A buffer solution containing 5 μM DNA and 50 μL rGO was stirred and incubated at room temperature for 15 min before each measurement.

4.5. Fluorescence Experiments. A buffer solution containing 5 μM DNA and ethidium bromide was stirred for 5 min, and then the measurements were performed. In the case of experiments with rGO, the buffer solution containing 5 μM DNA and 40 μL rGO was stirred for 15 min at room temperature, after which 5 μM ethidium bromide was added. The solution was further incubated for 5 min, and then the spectra were recorded.

■ ASSOCIATED CONTENT

Supporting Information

The Supporting Information is available free of charge on the ACS Publications website at DOI: 10.1021/acsomega.8b02063.

Cyclic voltammograms and CD spectra (PDF)

■ AUTHOR INFORMATION

Corresponding Author

*E-mail: jinheung@ewha.ac.kr. Tel: +82-2-3277-4453. Fax: +82-2-3277-3419.

ORCID

Jinheung Kim: 0000-0002-1003-3151

Notes

The authors declare no competing financial interest.

■ ACKNOWLEDGMENTS

This work was supported by the National Research Foundation (NRF) grant funded by the Korean government (NRF-2017R1A5A1015365 and NRF-2016R1A2B4012488) and "Next Generation Carbon Upcycling Project" (Project No. 2017M1A2A2042517) through the NRF funded by the Ministry of Science and ICT.

■ REFERENCES

(1) Katz, E.; Willner, H. Biomolecule-Functionalized Carbon Nanotubes: Applications in Nanobioelectronics. *ChemPhysChem* **2004**, *8*, 1084–1104.

(2) Niemeyer, C. M. Nanoparticles, Proteins, and Nucleic Acids: Biotechnology Meets Materials Science. *Angew. Chem., Int. Ed.* **2001**, *40*, 4128–4158.

(3) Tansil, N. C.; Gao, Z. Nanoparticles in Biomolecular Detection. *Nanotoday* **2006**, *1*, 28–37.

(4) Napier, M. E.; Hull, D. O.; Thorp, H. H. Electrocatalytic Oxidation of DNA-Wrapped Carbon Nanotubes. *J. Am. Chem. Soc.* **2005**, *127*, 11952–11953.

(5) Yang, R.; Tang, Z.; Yan, J.; Kang, H.; Kim, Y.; Zhu, Z.; Tan, W. Noncovalent Assembly of Carbon Nanotubes and Single-Stranded DNA: An Effective Sensing Platform for Probing Biomolecular Interactions. *Anal. Chem.* **2008**, *80*, 7408–7413.

(6) Kam, N. W. S.; O'Cennell, M.; Wisdom, J. A.; Dai, H. Carbon Nanotubes as Multifunctional Biological Transporters and Near-Infrared Agents for Selective Cancer Cell Destruction. *Proc. Natl. Acad. Sci. U.S.A.* **2005**, *102*, 11600–11605.

(7) Zheng, M.; Jagota, A.; Stano, M. S.; Santos, A. P.; Barone, P.; Chou, G. S.; Diner, B. A.; Dresselhaus, M. S.; Mclean, R. S.; Onoa, G. B.; Samsonidze, G. G.; Semke, E. D.; Usrey, M.; Walls, D. J. Structure-Based Carbon Nanotube Sorting by Sequence-Dependent DNA Assembly. *Science* **2003**, *302*, 1545–1548.

(8) Chang, H.; Tang, L.; Wang, Y.; Jiang, J.; Li, J. Graphene Fluorescence Resonance Energy Transfer Aptasensor for the Thrombin Detection. *Anal. Chem.* **2010**, *82*, 2341–2346.

(9) He, S.; Song, B.; Li, D.; Zhu, C.; Qi, W.; Wen, Y.; Wang, L.; Song, S.; Fang, H.; Fan, C. A Graphene Nanoprobe for Rapid, Sensitive, and Multicolor Fluorescent DNA Analysis. *Adv. Funct. Mater.* **2010**, *20*, 453–459.

(10) Lei, H.; Mi, L.; Zhou, X.; Chen, J.; Hu, J.; Guo, S.; Zhang, Y. Adsorption of Double-stranded DNA to Graphene Oxide Preventing Enzymatic Digestion. *Nanoscale* **2011**, *3*, 3888–3892.

(11) Wu, M.; Kempaiah, R.; Huang, P.-J. J.; Maheshwari, V.; Liu, J. Adsorption and Desorption of DNA on Graphene Oxide Studied by Fluorescently Labeled Oligonucleotides. *Langmuir* **2011**, *27*, 2731–2738.

(12) Umadevi, D.; Sastry, G. N. Quantum Mechanical Study of Physisorption of Nucleobases on Carbon Materials: Graphene versus Carbon Nanotubes. *J. Phys. Chem. Lett.* **2011**, *2*, 1572–1576.

(13) Tang, Z.; Wu, H.; Cort, J. R.; Buchko, G. W.; Zhang, Y.; Shao, Y.; Alsay, I. A.; Liu, J.; Lin, Y. Constraint of DNA on Functionalized Graphene Improves its Biostability and Specificity. *Small* **2010**, *6*, 1205–1209.

(14) Storhoff, J. J.; Lucas, A. D.; Garimella, V.; Bao, Y. P.; Muller, U. R. Homogeneous Detection of Unamplified Genomic DNA Sequences Based on Colorimetric Scatter of Gold Nanoparticle Probes. *Nat. Biotechnol.* **2004**, *22*, 883–887.

(15) Tan, W.; Wang, K.; Drake, T. J. Molecular Beacons. *Curr. Opin. Chem. Biol.* **2004**, *8*, 547–553.

(16) Tang, L.; Chang, H.; Liu, Y.; Li, J. Duplex DNA/Graphene Oxide Biointerface: From Fundamental Understanding to Specific Enzymatic Effects. *Adv. Funct. Mater.* **2012**, *22*, 3083–3088.

(17) Liu, J.; Cao, Z.; Lu, Y. Functional Nucleic Acid Sensors. *Chem. Rev.* **2009**, *109*, 1948–1998.

(18) Wu, Q.; Kang, H. K.; Oh, B. N.; Kim, J. Size-Dependent Interactions between Au Nanoparticles and DNA in Electrochemical Oxidation by Metal Complexes. *J. Phys. Chem. C* **2012**, *116*, 8020–8026.

(19) Katz, E.; Willner, I.; Wang, J. Electroanalytical and Bioelectroanalytical Systems Based on Metal and Semiconductor Nanoparticles. *Electroanalysis* **2004**, *16*, 19–44.

(20) Shipway, A. N.; Katz, E.; Willner, I. Nanoparticle Arrays on Surfaces for Electronic, Optical, and Sensor Applications. *ChemPhysChem* **2000**, *1*, 18–52.

(21) Johnston, D. H.; Glasgow, K. C.; Thorp, H. H. Electrochemical Measurements of Solvent Accessibility of Nucleobases Using Electron Transfer between DNA and Metal Complex. *J. Am. Chem. Soc.* **1995**, *117*, 8933–8938.

(22) Kim, J.; Kim, I. Y.; Choi, M. S.; Wu, Q. Label-free Electrochemical Detection of Adenosine Based on Electron Transfer from Guanine Bases in an Adenosine-Sensitive Aptamer. *Chem. Commun.* **2009**, 4747–4749.

(23) Thorp, H. H. Electrocatalytic DNA Oxidation. *Top. Curr. Chem.* **2004**, *237*, 159–181.

(24) Hughes, M. E.; Brandin, E. B.; Golovchenko, J. A. Optical Absorption of DNA–Carbon Nanotube Structures. *Nano Lett.* **2007**, *7*, 1191–1194.

(25) Choi, M. S.; Yoon, M.; Baeg, J.-O.; Kim, J. Label-free Dual Assay of DNA Sequences and Potassium Ions Using an Aptamer Probe and a Molecular Light Switch Complex. *Chem. Commun.* **2009**, 7419–7420.

(26) Zhao, C.; Qu, K.; Xu, C.; Ren, J.; Qu, X. Triplex Inducer-directed Self-assembly of Single-walled Carbon Nanotubes: A Triplex

DOI: 10.1021/acsomega.8b02063
ACS Omega 2018, 3, 15464–15470

DNA-based Approach for Controlled Manipulation of Nanostructures. *Nucleic Acids Res.* **2011**, *39*, 3939−3948.
(27) Liu, B.; Salgado, S.; Maheshwari, V.; Liu, J. DNA adsorbed on graphene and graphene oxide: Fundamental interactions, desorption and applications. *Curr. Opin. Colloid Interface Sci.* **2016**, *26*, 41−49.
(28) Hummers, W. S.; Offerman, R. E., Jr. Preparation of Graphitic Oxide. *J. Am. Chem. Soc.* **1958**, *80*, 1339.
(29) Park, S. J.; Kim, S.; Anjong, T. F.; Lee, S. E.; Kim, J. The Vital Role of Reduced Graphene Oxide in Enhanced Hydrogen Photoproduction with a Pyrene-pendant Rhodium Catalyst and Platinum Nanoparticles. *Carbon* **2015**, *94*, 448−454.
(30) Si, Y.; Samulski, E. T. Synthesis of Water Soluble Graphene. *Nano Lett.* **2008**, *8*, 1679−1682.

DOI: 10.1021/acsomega.8b02063
ACS Omega 2018, 3, 15464−15470